

# Effect of surface temperature on fuel retention and structure of Be-containing co-deposited layers

**Antti Hakola<sup>1</sup>, Kalle Heinola<sup>2,3</sup>, Kenichiro Mizohata<sup>3</sup>, Jari Likonen<sup>1</sup>, Cristian Lungu<sup>4</sup>, Corneliu Porosnicu<sup>4</sup>, Eduardo Alves<sup>5</sup>, Rodrigo Mateus<sup>5</sup>, Iva Bogdanovic Radovic<sup>6</sup>, Zdravko Siketic<sup>6</sup>, Vincenc Nemanic<sup>7</sup>, Mohit Kumar<sup>8</sup>, Cedric Pardanaud<sup>8</sup>, Pascale Roubin<sup>8</sup>, and EUROfusion WP PFC Contributors<sup>9</sup>**

<sup>1</sup> VTT, P. O. Box 1000, 02044 VTT, Finland

<sup>2</sup> Atomic and Molecular Data Unit, International Atomic Energy Agency, Vienna, Austria

<sup>3</sup> Department of Physics, University of Helsinki, P. O. Box 64, 00014 University of Helsinki, Finland

<sup>4</sup> National Institute for Laser, Plasma and Radiation Physics, Magurele, Bucharest, Romania

<sup>5</sup> Instituto Superior Técnico, Universidade de Lisboa, Bobadela, Portugal

<sup>6</sup> Rudjer Boskovic Institute, P. O. Box 180, 10002 Zagreb, Croatia

<sup>7</sup> Jozef Stefan Institute, Jamova Cesta 39, 1000 Ljubljana, Slovenia

<sup>8</sup> Aix Marseille Université, CNRS, PIIM UMR 7345, 13397 Marseille, France

<sup>9</sup> See the author list in "S. Brezinsek et al 2017 Nucl. Fusion **57** 116041"

E-mail: antti.hakola@vtt.fi

Received xxxxxx

Accepted for publication xxxxxx

Published xxxxxx

## Abstract

We have investigated retention of plasma fuel in beryllium-containing, laboratory-made films whose properties resemble co-deposits observed on JET-ILW or predicted for ITER. The best correspondence of the produced layers to JET-ILW results in terms of composition, surface properties, and fuel (deuterium) retention and release characteristics is obtained by preparing the layers using high-power impulse magnetron sputtering and keeping the sample temperature at 100-200°C during the deposition phase. We notice that carbon impurities play a large role in explaining the reported D concentrations of ~5 at.% in JET-ILW-like deposits. This we attribute to material defects as well as aliphatic and aromatic C-D bonds. Other impurities do not significantly alter the D inventory while increased surface roughness leads to enhanced retention. The results from Be-D layers with and without gaseous impurities indicate that fuel retention in ITER-like co-deposits would be around 1-2 at.%.

Keywords: beryllium, fuel retention, co-deposition

## 1. Introduction

Beryllium (Be) will be used as a plasma-facing material in the main chamber of ITER [1]. To lay the basis for efficient operation of ITER in the late 2020s, JET has been equipped with an ITER-Like Wall (ILW), consisting of a Be main chamber and a tungsten (W) divertor [2]. Two important aims of the ILW project are estimating material migration and fuel retention in an ITER-relevant environment, and this has now been carried out during three successive campaigns.

Compared to operations in the carbon phase, fuel retention in JET-ILW is reduced by a factor of 10-20 and is dominated by co-deposition [3, 4]. Up to 40 µm thick layers are predominantly formed on the high-field side (inner) divertor plasma-facing components (PFCs) [5-7] and the deposits are rich in Be, fuel (here deuterium (D)) and impurities (e.g., oxygen (O) and nitrogen (N)) [5-7].

The observations call for understanding how fuel is accumulating in co-deposits, and this is best met by systematic production of laboratory samples whose properties can be tailored over a wide range of parameters. Such layers have

already been produced for plasma experiments in laboratories [8, 9] and in linear plasma devices, most noticeably in PISCES-B [10-14]. Several trends for the dependence of retention on, e.g., the properties of the incoming plasma and the sample material have been reported but identifying how fuel is retained in a growing layer has attracted less attention.

Here we investigate the physical mechanisms that contribute to the observed large retention in JET-ILW layers and that would allow making predictions for ITER and future fusion reactors. To this end, layers with different compositions, fuel contents, thicknesses, and surface morphologies have been produced within an extensive development project under the EUROfusion Consortium.

## 2. Production and analyses of the co-deposited layers

All the samples were produced in the National Institute for Laser, Plasma and Radiation Physics in Romania, mainly using High Power Impulse Magnetron Sputtering (HiPIMS) [15], which resulted in good control of composition, thickness, surface quality, and fuel content of the samples. The studied sample types were Be-D (expected composition for typical co-deposits on ITER PFCs), Be-O-D and Be-N-D (examples of impurity-containing deposits), and Be-C-O-D (mimicking co-deposits on the JET-ILW apron region [6]). In addition, a number of Be-W-D films with different surface roughnesses were prepared to simulate mixed deposits in ITER. For these layers, Thermo-Vacuum Arc (TVA) deposition [16] was applied. The surface roughness was altered by changing the bias voltage of the samples during their preparation.

Both in TVA and HiPIMS separate targets were used for all the metallic elements (Be, W, C), while different gases (D, O, N) were injected into the deposition chamber such that the total pressure ranged from 0.7 to 3.0 Pa [17]. The goal values for the C, N, and O impurities were 5-10 at.% while the desired fuel (D) content was in the range of 1-10 at.%. In Be-W-D layers, the Be:W ratios were set to 1:0, 2:1, 1:1, 1:2, and 0:1 and the D content to ~1 at.%.

The production recipes were optimized by varying the source parameters, gas flows, and the deposition geometry. Moreover, the surface during the production phase was either kept at room temperature or heated to 100, 200, 400, or 600°C. The films were produced on Si and W substrates and their thickness ranged from 0.4 to 15  $\mu\text{m}$ . In TVA, the deposition geometry was kept fixed while in HiPIMS, two different variants were applied. In the standard one (called *setup 1*), one Be source at 45° to the substrate was used and the duration of the magnetron pulsed was varied for the different deposition fluxes. Carbon impurities were introduced to the growing film from a single target, also at 45°, by applying direct-current sputtering [17]. All this resulted in slightly varying magnetron plasmas at the sample plane from one deposition run to another. In *setup 2*, instead, three Be sources at 30° and a single C source perpendicular to the substrate were used. Now

the deposition flux was adjusted by varying the repetition rate of the magnetron pulses, thus making the plasmas between various deposition batches comparable [17]. In both *setup 1* and 2, the electron density was  $n_e \sim 10^{18} - 10^{19} \text{ m}^{-3}$ , the electron temperature  $T_e \sim 2 - 5 \text{ eV}$ , and the typical ion energies 1-10 eV with high-energy tails up to 60 eV in the case of Be and 500 eV for D [17].

After the production, the samples were analyzed in different contributing laboratories for their actual properties. Rutherford Backscattering Spectrometry (RBS), Nuclear Reaction Analysis (NRA), Time-of-flight Elastic Recoil Detection Analysis (TOF-ERDA), Secondary Ion Mass Spectrometry (SIMS), Thermal Desorption Spectroscopy (TDS), and Raman spectroscopy were used. Complementary information was provided by Atomic Force Microscopy (AFM) and Scanning Electron Microscopy (SEM) analyses. Typically, composition and thickness were extracted from RBS, TOF-ERDA, and SIMS data, fuel retention by combining the results from NRA, TOF-ERDA, TDS, and SIMS measurements, and indications for retention mechanisms were concluded from the features in the NRA, TDS, and Raman spectra.

## 3. Results

### 3.1 Effect of composition on retention

The first sets of samples were produced at room temperature to optimize the deposition parameters for film compositions. The measured fuel content followed the applied D gas flow but was generally higher than the goal of 1-10 at.%. The impurity (C, O, N) concentrations, for their part, were in line with the target level of 5-10 at.%. The retention data for a number of samples from different deposition batches (thickness 5-15  $\mu\text{m}$ ), produced using both *setup 1* and 2, are shown as a function of the target D concentration in Figure 1.

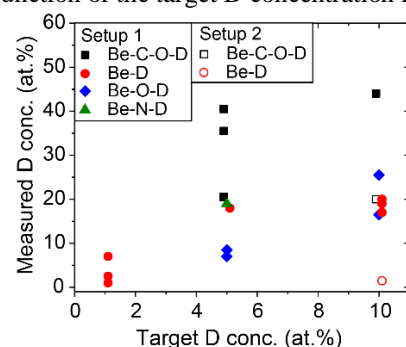


Figure 1. Measured D retention as a function of target value for D concentration in different Be-based samples. Data is extracted from NRA, TOF-ERDA, and TDS measurements.

A clear difference can be noticed between the properties of samples produced using *setup 1* and *setup 2*. In the latter case, better control of plasma parameters and the deposition flux have resulted in the retention to drop significantly: for the

target D content of 10 at.%, the measured D concentrations decrease from ~45 at.% to ~20 at.% in the case of Be-C-O-D samples and from ~20 at.% to ~2 at.% for Be-D samples. This trend indicates the deposits originating from *setup 2* to have a uniform and dense structure. The second key observation is that the inclusion of carbon in the compound increases retention by almost an order of magnitude; the largest D inventories are measured for samples with C concentrations >10 at.%. In contrast, other impurities do not have a noticeable effect on retention, but the addition of O may even decrease D accumulation.

The results can be, at least partly, explained by the results of Raman spectroscopy. The recorded data show that samples produced using *setup 2* contain fewer defects than those prepared using *setup 1*, suggesting that improving the uniformity of Be (and C) fluxes during the deposition of the samples drastically reduces their defect concentration. Consequently, fewer trapping sites are left for D as observed in Figure 2a and already reported in [18]: for samples produced using the *setup 2* geometry, the contribution of defects to the Raman spectrum is almost non-existent and bonding as D<sub>2</sub> molecules is also diminished compared to the case of *setup 1*. For Be-O-D samples, the results are in line with the Be-D data but the peaks are generally weaker.

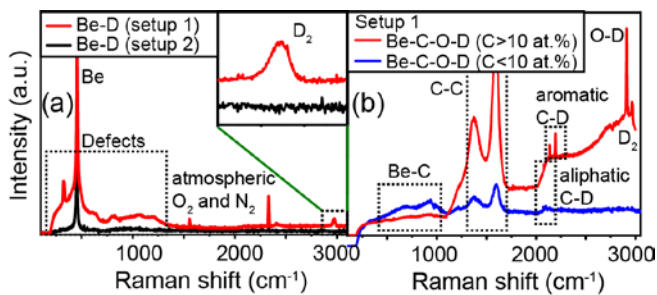


Figure 2. Raman spectra extracted from (a) Be-D and (b) Be-C-O-D samples using 325 nm laser light. In (b) the data is exclusively from samples produced using *setup 1*.

In Be-C-O-D, both beryllium carbide and aromatic carbon are present, and contribution to fuel retention is evidenced by the presence of aliphatic and aromatic C-D bonds. Moreover, when the aromatic C-C signal is the most prominent, aromatic C-D bonding becomes clearly distinguishable. Generally, these correlate well with the measured C content of the sample to exceed > 10 at.%. Figure 2b shows also peaks associated to D<sub>2</sub> and O-D bonds [25] especially for the samples with C concentrations >10 at.%. Instead, no clear signs of Be-D bonds are visible, probably due to the absence of stoichiometric BeD<sub>2</sub> [19].

Raman measurements also give indications on the crystal structure of the films. In Be-D and Be-O-D, a band is typically observed close to 450 cm<sup>-1</sup>, and according to previous studies in [20], it is a signature of the atoms being arranged close to that of a Be crystal. In contrast, in Be-C-O-D, the signature for

Be crystallites is faint. This indicates impurities to also influence the crystallinity of the growing deposit.

The thickest (>5 μm) films with the highest Be fractions are susceptible to exfoliation due to stresses building up in the layers. This is attributed to increasing crystallinity of the films as discussed above: films with high amounts of impurities show relatively good adhesion to their substrates. Another parameter affecting the relief of stresses and stability of the forming film is the deposition temperature, which will be discussed in the following section.

### 3.2 Effect of surface temperature on retention

Heating the surface during deposition resembles the conditions during flat-top phases of plasma discharges. With this in mind, a series of Be-D and Be-C-O-D samples at different temperatures (see Section 2) were produced using *setup 2*. The resulting D concentrations for 10-15-μm thick samples, as extracted from TOF-ERDA measurements, are collected in Figure 3. One can see that retention drops by an order of magnitude as the deposition temperature increases from room temperature to 600°C and that the most dramatic changes occur above 200°C. At the highest temperatures, D concentrations in Be-D and Be-C-O-D become comparable but relatively low. Again, we attribute the observations to modified trap and defect configurations, assisted by weaker bonding of D as D<sub>2</sub>, O-D, or C-D; Such features are absent in the measured Raman spectra. According to SIMS measurements, also the depth profiles of deuterium are drastically different at low and high temperatures: below 200°C, the profiles are uniform throughout the entire layer whereas at higher temperatures D is retained in a 0.1-1-μm thick surface layer. Data from PISCES-B [10, 12] support our findings: retention in Be and Be-O layers decreases dramatically as temperature increases above 100°C.

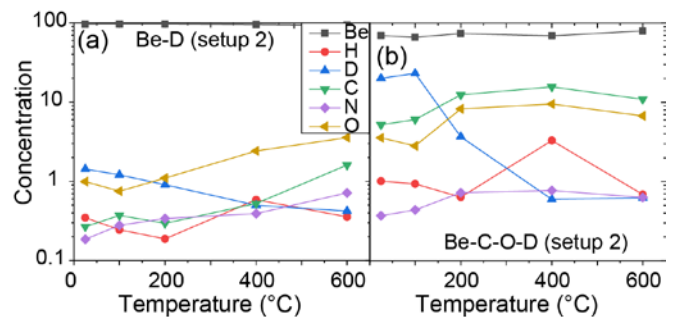


Figure 3. TOF-ERDA results for different elements in (a) Be-D and (b) Be-C-O-D layers produced at different surface temperatures. The samples are from batches produced using *setup 2*.

The TDS analyses, whose results are shown in Figure 4 separately for Be-D and Be-C-O-D layers, reveal another important effect of the increased deposition temperature: the hotter the surface during the film production, the more likely will high-temperature traps for D be populated. This becomes

evident as the main release peak of D is shifted from 300–500°C to >600°C when the deposition temperature is increased from room temperature to 200°C. The data agrees with the results reported for JET-ILW samples in [21].

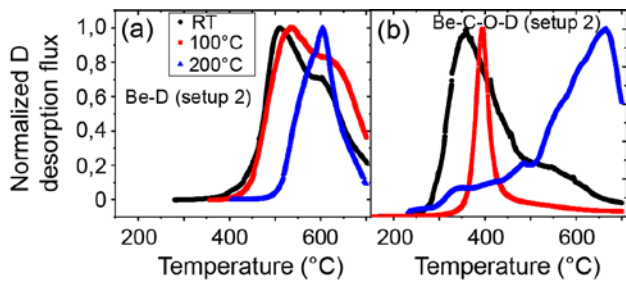


Figure 4. TDS data on normalized D desorption flux for (a) Be-D and (b) Be-C-O-D layers produced using different surface temperatures and applying setup 2.

At higher surface temperatures, the exfoliation effects mentioned in Section 3.1 are almost non-existent, pointing towards relief of stresses during the high-temperature “annealing” phase. This gives additional proof that elevated surface temperatures are crucial in explaining the features of tokamak co-deposits.

### 3.3 Effect of layer thickness and surface characteristics on retention

As the thickness of the produced samples exceeds 1  $\mu\text{m}$ , their D levels increase by a factor of 5–10 compared to thinner variants of the same sample type. This is illustrated in Figure 5 where TOF-ERDA depth profiles of H, D, Be, C, O, and N for a  $\sim 0.4 \mu\text{m}$  (part a) and  $\sim 5.5 \mu\text{m}$  (part b, data from the 0.5  $\mu\text{m}$  thick surface layer) thick, otherwise comparable Be-C-O-D samples prepared using *setup 1*, are shown. The differences can be associated with fewer defects in thinner films, to chemical reactions in the pre-cursor phase of the deposit, and to a shorter escaping distance for retained D as the layer thickness is only some hundreds of nm. Such observations are supported by experiments made in PISCES-B for samples with varying thickness [11].

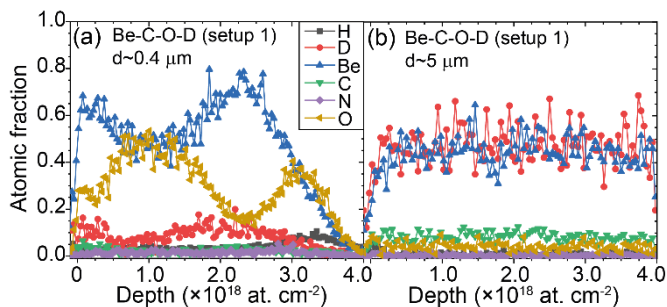


Figure 5. TOF-ERDA depth profiles within a  $\sim 500\text{-nm}$  thick surface layer for Be-C-O-D samples produced using *setup 1* and with thicknesses of (a) 400 nm and (b) 5  $\mu\text{m}$ .

Figure 5 also shows another interesting feature: the smaller the O content, the higher is the D retention in the coatings. However, this seems to be valid only for thin layers (Figure 5a) and for cases where the O concentration is >20 at.%. For thick coatings and O levels around 5–10 at.%, no clear correlation with retention is observed as the data in Section 3.1 proves. Possible explanation is related to the oxidation of Be which reduces the number of trapping sites for D as the oxygen levels increase beyond the level of a small impurity.

The produced Be-C-O-D, Be-O-D, and Be-D samples have generally a smooth surface, almost independent of their D content, and the irregularities on the surface reflect those of the substrate. Compared to tokamak PFCs, the measured surface roughness of  $R_a < 100 \text{ nm}$  is orders of magnitudes smaller. Detailed investigations of a set of Be-W-D samples with different Be:W ratios and inherent surface morphologies [22] have revealed that surface roughness has an effect on retention: when the roughness increases by two orders of magnitude (from  $< 1 \text{ nm}$  to  $\sim 100 \text{ nm}$ ), retention increases but only by a factor of  $\sim 1.5$ . This we can see in Figure 6. According to AFM analyses, rough surfaces consist to a large extent of hills and valleys with heights up to 500 nm, and such a terrain favours accumulation of D on the surface. Comparable samples without D inclusions were exposed to plasmas in PISCES-B and they exhibited a similar but a clearer trend with retention increasing by a factor of 5 for pure Be compared to mixed Be-W deposits and the surfaces becoming strongly modified due to plasma exposure [12].

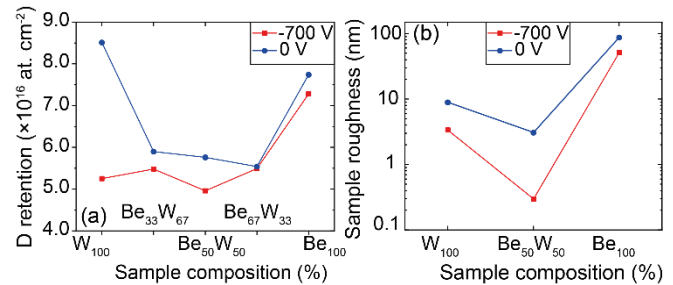


Figure 6. (a) Measured D retention for various Be-W-D layers and for different bias voltages during the sample production. (b) Measured roughness for selected Be-W-D layers of part (a).

### 3.4 Comparison to deposits obtained from JET-ILW

Comparison of results from Be-C-O-D layers, reported in the previous sections, with published data from the apron region of JET-ILW [6] are summarized in Table 1. Here the elemental composition of both samples is shown, in the case of Be-C-O-D for deposits produced at 200°C using HiPIMS *setup 2*. One can notice the good correspondence between the elemental compositions of the laboratory-made co-deposits and the JET-ILW layers. Also the conditions during deposition are similar to those measured in the JET-ILW divertor. Most noticeably, the particle energies and plasma parameters on the samples are comparable as discussed in

Section 2. The optimal surface temperature window of 100-200°C during sample preparation also agrees with the data from JET-ILW apron: the base temperature is  $T_{\text{base}}=90\text{-}120^\circ\text{C}$  and during plasma discharges can rise by  $\Delta T=150^\circ\text{C}$  [23].

Table 1. Composition of JET-ILW co-deposits and laboratory samples produced using optimized deposition conditions.

Element	JET-ILW [5]	Co-deposits (>5 $\mu\text{m}$ , T=200 °C)
Be	75-85 at. %	70-80 at. %
C	3-10 at. %	10-15 at. %
O	6-9 at. %	5-10 at. %
D	4-5 at. %	3-5 at. %

Despite the good agreement there are still some discrepancies in the finer details, including the TDS release peaks being much broader in the case of JET-ILW samples, the emergence of more complicated bonds [24] than those reported in Section 3.1 for the lab-made co-deposits, and the persistently remaining D inventories in the JET-ILW samples even after heating them to 350°C [7]. Possible reasons for the deviations are the high surface roughness of JET-ILW PFCs ( $R_a$  up to 10  $\mu\text{m}$ ) and the JET-ILW samples being exposed to complicated temperature excursions during the formation of the deposits, all introducing additional retention mechanisms to those identified above.

The retained D depth profile in JET-ILW specimens is not constant throughout the samples, but has a noticeable near-surface peak extending to depths of tens of nm followed by a lower concentration profile extending deep in the bulk of several  $\mu\text{m}$  [6]. The near-surface D may be easily released and hence seen as a sharp peak in the TDS spectrum at low temperatures. The depth dependence of D concentration profile to the release dynamics will be addressed using new dedicated samples

#### 4. Discussion and conclusions

We have investigated retention of plasma fuel in beryllium-based, laboratory-made films whose properties resemble co-deposits observed on JET-ILW or predicted for ITER. The prepared samples consisted of D-doped Be, Be-O, and Be-C-O layers, in addition to which D-containing Be-W deposits with varying Be:W ratios were produced.

The best correspondence to JET-ILW results in terms of composition, surface characteristics, and the D content of the produced layers, as well as their retention and release behaviour, is obtained by heating the samples to 100-200°C during the deposition phase. In addition, carbon was noticed to play a large role in explaining the large D concentrations of ~5 at.% in JET-ILW-like Be-C-O-D deposits. This we attribute to deuterium being bound to defects of the produced layer as well as efficient bonding as C-D, O-D, and D<sub>2</sub> molecules in the layer. Surface roughness or otherwise

strongly modified surface increases retention but in the studied regime only a factor of 1.5 increase in D inventory was measured following a roughness increase by some two orders of magnitude.

The results from ITER-relevant Be-D coatings with and without gaseous impurities (O, N) indicate that retention in such layers would be around 1-2 at.%, thus being not so dominant as in JET-ILW deposits. However, the release behaviour of fuel from such layers is still to be investigated to see if hydrogen isotopes are as stubbornly caught in Be-D as they are in Be-C-O-D upon exposure to ITER-like baking cycles. Moreover, the effect of realistic temperature excursions during plasma discharges on retention are to be addressed, as well as the role of roughness, complex impurity combinations, and various isotopic ratios (with H and D) in D accumulation. All these are topics of our future investigations.

#### Acknowledgements

This work has been carried out within the framework of the EUROfusion Consortium and has received funding from the Euratom research and training programme 2014-2018 and 2019-2020 under grant agreement No 633053. The views and opinions expressed herein do not necessarily reflect those of the European Commission. Work performed under EUROfusion WP PFC

#### References

- [1] Pitts R A *et al* 2007 *J. Nucl. Mater.* **415** S957.
- [2] Matthews G F *et al* 2013 *J. Nucl. Mater.* **438** S2.
- [3] Brezinsek S *et al* 2013 *Nucl. Fusion* **53** 083023.
- [4] Brezinsek S and JET-EFDA contributors 2015 *J. Nucl. Mater.* **463** 11.
- [5] Mayer M *et al* 2017 *Phys. Scr.* **T170** 014058.
- [6] Heinola K *et al* 2017 *Phys. Scr.* **T170** 014063.
- [7] Heinola K *et al* 2017 *Nucl. Fusion* **57** 086024.
- [8] Sugiyama K *et al* 2016 *Nucl. Mater. Energy* **6** 1.
- [9] Sugiyama K *et al* 2013 *J. Nucl. Mater.* **438** S1113.
- [10] De Temmerman G *et al* 2008 *Nucl. Fusion* **48** 075008.
- [11] Baldwin M J and Doerner R P 2014 *Nucl. Fusion* **54** 083032.
- [12] Jepsu I *et al* 2015 *J. Nucl. Mater.* **463** 983.
- [13] Roth J *et al* 2013 *J. Nucl. Mater.* **438** S1044.
- [14] Dittmar T *et al* 2013 *J. Nucl. Mater.* **438** S988.
- [15] Dinca P *et al* 2017 *Surf. Coat. Technol.* **321** 397.
- [16] Lungu C P *et al.* 2007 *Phys. Scr.* **T128** 157.
- [17] Dinca P *et al* 2019 *Surf. Coat. Technol.* **363** 273.
- [18] Pardanaud C *et al* 2015 *J. Phys.: Condens. Matter* **27** (2015) 475401.
- [19] Pardanaud C *et al* 2016 *Phys. Scr.* **T167** (2016) 014027.
- [20] Rusu M I *et al* 2017 *Nucl. Fusion* **57** 066035.
- [21] Likonen J *et al* 2019 *Nucl. Mater. Energy* **19** 300.
- [22] Mateus R *et al* 2017 *Fusion Eng. Design* **124** 464.
- [23] Brezinsek S *et al* 2016 *Phys. Scr.* **T167** 014076.
- [24] Kumar M *et al* 2018 *Nucl. Mater. Energy* **17** 295